Electronic Supplementary Information

PtPd hollow nanocubes with enhanced alloy effect and active facets for efficient methanol oxidation reaction

Yu-Xuan Xiao,[a] Jie Ying,[*b] Ge Tian,[a] Xue-Qi Zhang,[a] Christoph Janiak,[c] Kenneth I. Ozoemena[d] and Xiao-Yu Yang[*abe]

[a] *State Key Laboratory of Advanced Technology for Materials Synthesis and Processing & School of Materials Science and Engineering, Wuhan University of Technology, 122, Luoshi Road, Wuhan 430070, China.*

[b] *School of Chemical Engineering and Technology, Sun Yat-sen University (SYSU), (Guangdong, Zhuhai) & Southern Marine Science and Engineering Guangdong Laboratory (Zhuhai), Zhuhai, 519000, China.*

[c] *Institut für Anorganische Chemie und Strukturchemie, Heinrich-Heine-Universität Düsseldorf, 40204 Düsseldorf, Germany.*

[d] *Molecular Sciences Institute, School of Chemistry, University of the Witwatersrand, Private Bag 3, Johannesburg 2050, South Africa.*

[e] *School of Engineering and Applied Sciences, Harvard University, Cambridge, Massachusetts 02138, USA.*

*Corresponding author. E-mail: xyyang@whut.edu.cn; yingj5@mail.sysu.edu.cn; xyyang@seas.harvard.edu

Author Contributions

Y. X. X. and X. Q. Z. did the experiments of synthesis and electrocatalytic performance. J. Y. and X. Y. Y. conceived the project, provided the idea, and designed the experiments. G. T. performed the TEM and EDS characterizations. Y. X. X., J. Y. and X. Y. Y. wrote and revised the paper. C. J. and K. I. Q. revised the paper. All the authors discussed results and analyzed the data, and have given approval to the final version of the manuscript.

Experimental section

1. Materials

Na_2PdCl_4, $H_2PtCl_6 \cdot 6H_2O$, N,N-dimethylformamide (DMF), KOH, and KI were purchased from Shanghai Aladdin Biochemical Polytron Technologies Inc. Polyvinylpyrrolidone (PVP, Mw ≈ 55,000 g/mol) was purchased from Sigma-Aldrich. Ethanol, acetone, and concentrated nitric acid (65.0～68.0%) were purchased from Sinopharm Chemical Reagent Co., Ltd. Commercial Pt/C (20 wt% Pt) was purchased from Johnson Matthey Corp. Commercial carbon black (Vulcan-XC 72R) was purchased from Shanghai Cabot Co., Ltd. All chemical reagents were used as received without further purification. De-ionized (DI) water (18.2 MΩcm) was used throughout.

2. Synthesis of Pd nanocubes

In a typical synthesis, 300 mg KI and 640 mg PVP were added to a flask of 100 mL, then 4 mL of 20 mM Na_2PdCl_4 and 40 mL DMF were added and stirred until the solution became homogeneous. The solution was heated in an oil bath of 140 ℃ for 2 h under stirring. After that, the Pd nanocubes were collected by centrifugation at 12,000 rpm for 10 min, washed with 10 mL each of an ethanol/acetone (volume ratio of 1:1) mixture for three times, and dispersed in 4 mL of DMF.

3. Synthesis of PtPd HNCs

PtPd HNCs were synthesized by using Pd nanocubes as templates. Typically, 300 mg KI and 640 mg PVP were added to a flask of 100 mL, then 4 mL of the Pd nanocube dispersion in DMF (see above), 4 mL of 20 mM $H_2PtCl_6 \cdot 6H_2O$, and 36 mL of DMF were added and stirred until the solution became homogeneous. The solution was heated in an oil bath of 140 ℃ for 2 h under stirring. After that, the PtPd HNCs were collected by centrifugation at 12,000 rpm for 10 min, washed with 10 mL each of an ethanol/acetone (volume ratio of 1:1) mixture for three times.

4. Synthesis of PtPd HNCs-E

PtPd HNCs-E were obtained by selective chemical etching of Pd from PtPd HNCs. The amount of 20 mL of concentrated nitric acid (65.0～68.0%) was added to the as-prepared PtPd HNCs and the etching process was kept for 5 days. The PtPd HNCs-E were collected by centrifugation at 12,000 rpm for 10 min, washed with 10 mL each of H_2O several times until the pH of the solution was close to 7.

5. Physical characterization

Transmission electron microscopy (TEM), high-angle annular dark field scanning transmission electron microscopy (HAADF-STEM) and energy-dispersive X-ray spectroscopy (EDX) analyses were conducted with a Talos F200S (Thermo Fisher, USA) in Wuhan University of Technology. X-ray diffraction (XRD) measurements were performed on a Bruker D8-Advance X-ray diffractometer operating with Cu Kα radiation (λ=1.54056 Å). The X-ray photoelectron spectroscopy (XPS) measurements were carried out by an ESCALAB 250Xi (Thermo Fisher, USA). The samples of PtPd HNCs-E and PtPd HNCs were loaded on carbon black for XPS measurement for a better comparison with commercial Pt/C. The zeta potentials of the samples were measured using a zeta potential analyser (Brookhaven Instruments Co, USA). During the measurements, the samples were suspended in DI water at very low concentrations to make sure that the pH of each system remained unchanged. The content analyses of Pt and Pd were measured by inductively coupled plasma-atomic emission spectrometry (ICP-AES, Prodigy 7, LEEMAN LABS INC, USA).

6. Electrochemical measurements

A three-electrode cell was used for the electrochemical measurements on an Autolab working station from Metrohm, Switzerland. An Ag/AgCl (3 M) electrode was used as a reference electrode, a platinum mesh as a counter electrode, and a glassy-carbon electrode (diameter: 5 mm, area: 0.196 cm^2) as the working electrode. Before tests, PtPd HNCs-E and PtPd HNCs were supported by commercial carbon black. The loading amount of the catalysts on the electrode were 10 μg. The cyclic voltammetry (CV) measurements were performed in 0.1 M KOH, and methanol oxidation reaction (MOR) measurements were carried out in 0.1 M KOH + 1 M CH_3OH solution at a sweep rate of 50 mV/s. Chronoamperometry measurements were performed in 0.1 M KOH + 1 M CH_3OH at 0.8V versus a reversible hydrogen electrode (RHE). CO stripping experiments were conducted by first introducing CO gas to the three-electrode cell for 30 min, holding the potential of the working electrode at 0.1 V (RHE), and then introducing nitrogen gas for 30 min to remove CO from the electrolyte. After that, CO was stripped using CV performed in a potential range at a sweep rate of 50 mV s^{-1}. The accelerated durability tests (ADTs) were performed in 0.1 M KOH solution with cyclic potential sweeps between 0.6 and 1.1 V (RHE) at a 50 mV/s sweep rate for 6000 cycles at room temperature.

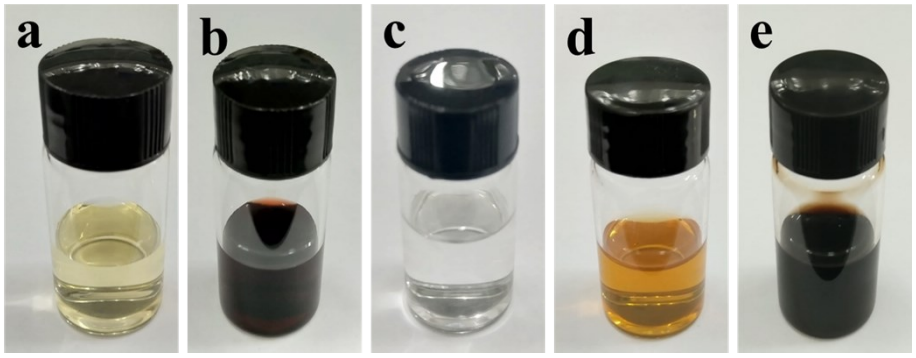

Fig. S1. Optical photographs of (a) 0.5 mL 20 mM $H_2PtCl_6 \cdot 6H_2O$ + 5 mL DMF, (b) 0.5 mL 20 mM $H_2PtCl_6 \cdot 6H_2O$ + 5 mL DMF + 25 μL 5 M KI, (c) 5M KI, (d) 0.5 mL 20 mM Na_2PdCl_4 + 5 mL DMF, and (e) 0.5 mL 20 mM Na_2PdCl_4 + 5 mL DMF + 25 μL 5 M KI.

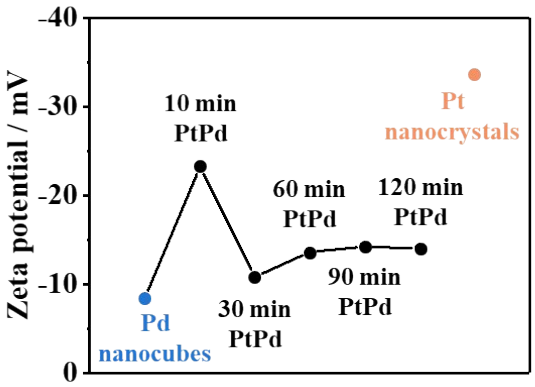

Fig. S2. Zeta potential values for the synthesis of PtPd HNC with different reaction time.

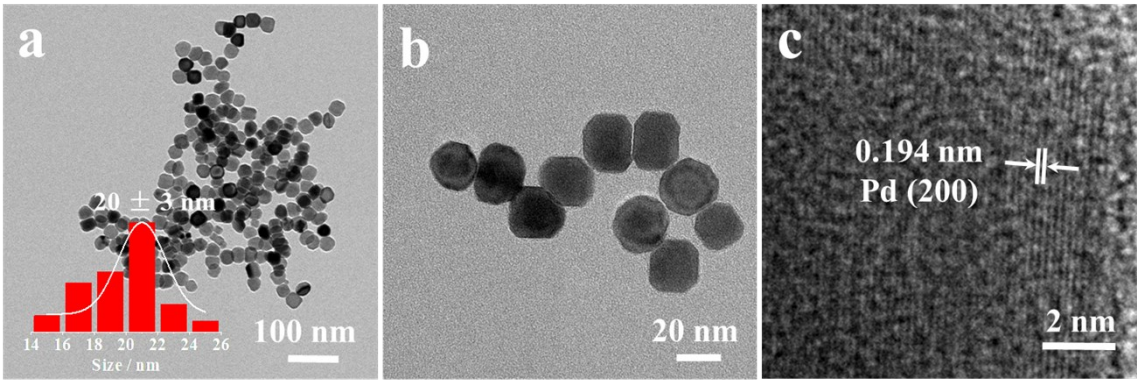

Fig. S3. TEM images of Pd nanocubes with (a) low and (b) high magnification. The inset in (a) is the corresponding particle size distribution. (c) Lattice fringes of Pd nanocubes.

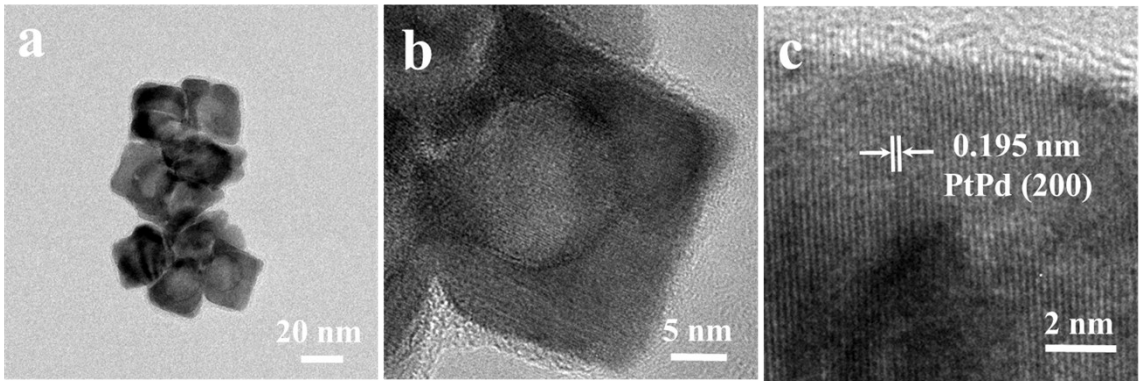

Fig. S4. TEM images of PtPd HNCs with (a) low and (b) high magnification. (c) Lattice fringes of PtPd HNCs.

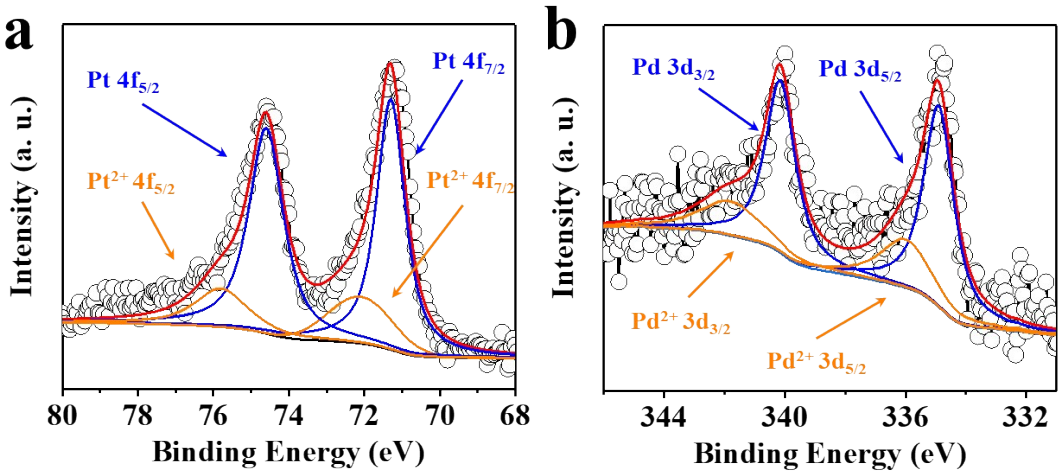

Fig. S5. Peak fitting results of (a) Pt 4f and (b) Pd 3d XPS signal of PtPd HNCs.

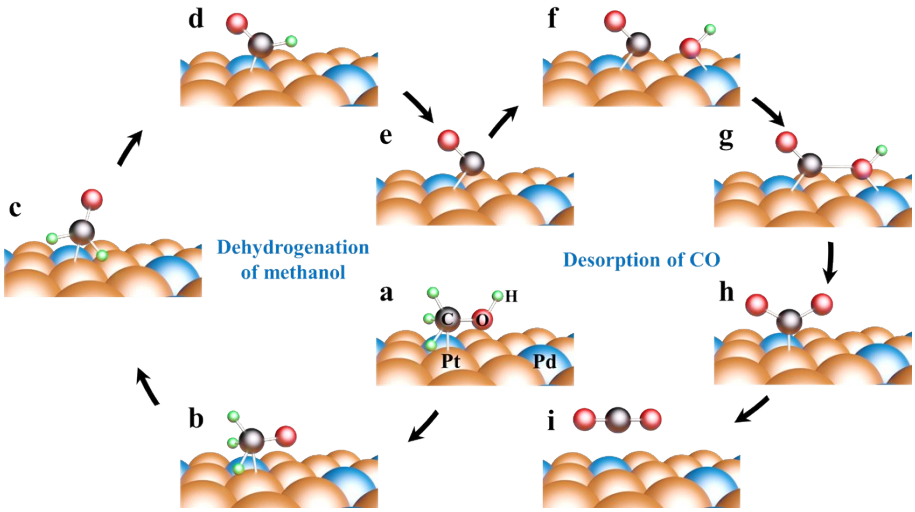

Fig. S6. Schematic depiction of possible methanol oxidation mechanism on PtPd alloy surface. (a) Absorption of methanol molecule (CH_3OH_{ads}) on Pt atom. (b) Formation of CH_3O_{ads} on Pt atom. (c) Formation of CH_2O_{ads} on Pt atom. (d) Formation of CHO_{ads} on Pt atom. (e) Formation of CO_{ads} on Pt atom. (f) Formation of OH_{ads} on Pd atom. (g) Bonding of CO_{ads} and OH_{ads}. (h) Formation of CO_{2ads} on Pt atom. (i) Desorption of CO_2 from Pt atom.

The electrooxidation of methanol on PtPd catalyst can be decomposed into two parts. Firstly, methanol molecules will be absorbed on the surface of Pt atoms, and gradually dehydrogenated to CO_{ads} (Fig. S6a-e). The adsorbed CO_{ads} would be scarcely stripped out until the oxygen-containing species (OH_{ads}) is generated on the Pt surfaces under high electrode potential. However, the additional Pd atoms can provide adsorbed OH_{ads} at a lower potential (Fig. S6f), which serve as the oxidant to finally effectively oxidize the CO_{ads} to CO_2 and desorbed from Pt atom (Fig. S6g-i).

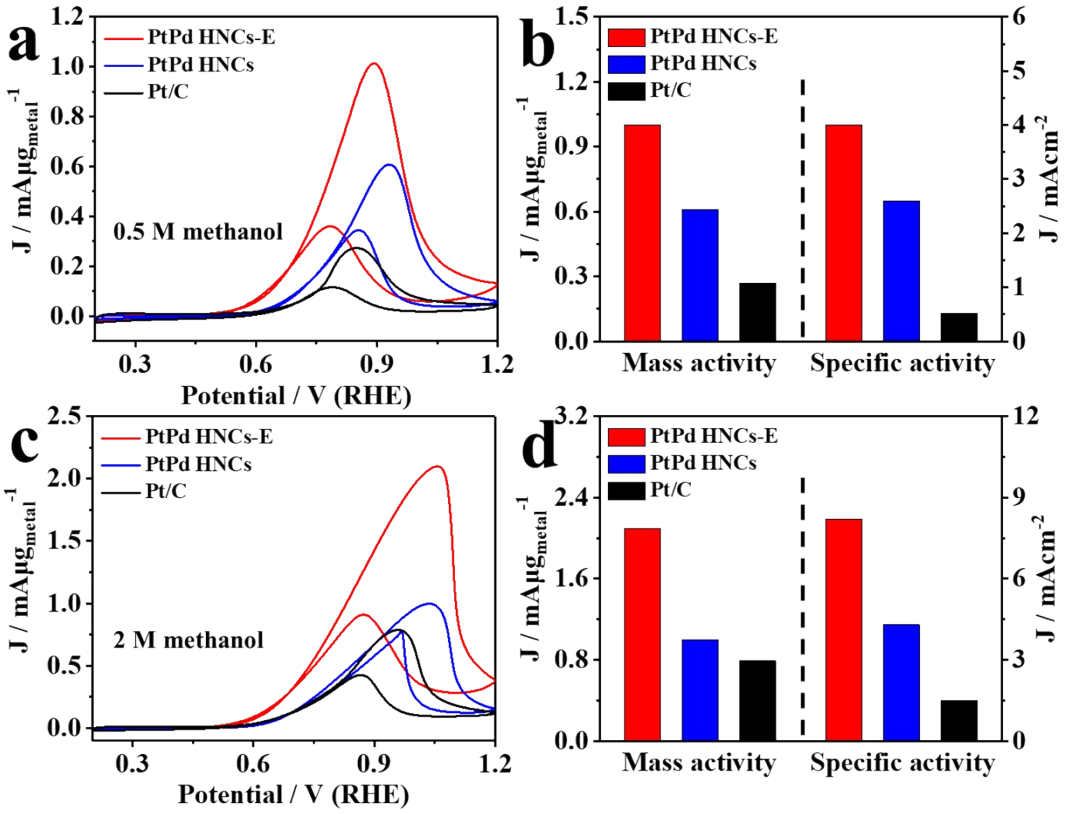

Fig. S7. (a) CV curves recorded in 0.1 M KOH + 0.5 M CH_3OH and (b) corresponding mass activity and specific activity of PtPd HNCs-E, PtPd HNCs, and commercial Pt/C. (c) CV curves recorded in 0.1 M KOH + 2 M CH_3OH and (d) corresponding mass activity and specific activity of PtPd HNCs-E, PtPd HNCs, and commercial Pt/C.

The MOR performance of catalysts with different methanol concentration was explored and shown in Fig. S7. Fig. S7a shows the CV curves of PtPd HNCs-E, PtPd HNCs, and commercial Pt/C recorded in 0.1 M KOH + 0.5 M CH_3OH. As summarized in Fig. S7b, PtPd HNCs-E exhibited a mass activity of 1.0 mA μg_{metal}^{-1}, which is 1.6 and 3.7 times than that of PtPd HNCs (0.61 mA μg_{metal}^{-1}) and commercial Pt/C (0.27 mA μg_{metal}^{-1}). Moreover, the specific activity of PtPd HNCs-E was 4.0 mA cm^{-2}, which is 1.5 and 7.7 times than that of PtPd HNCs (2.6 mA cm^{-2}) and commercial Pt/C (0.52 mA cm^{-2}). Fig. S7c shows the CV curves of PtPd HNCs-E, PtPd HNCs, and commercial Pt/C recorded in 0.1 M KOH + 2 M CH_3OH. As shown in Fig. S7d, PtPd HNCs-E exhibited a mass activity of 2.1 mA μg_{metal}^{-1}, which is 2.1 and 2.7 times than that of PtPd HNCs (1.0 mA μg_{metal}^{-1}) and commercial Pt/C (0.79 mA μg_{metal}^{-1}). Moreover, the specific activity of PtPd HNCs-E was 8.2 mA cm^{-2}, which is 1.9 and 5.5 times than that of PtPd HNCs (4.3 mA cm^{-2}) and commercial Pt/C (1.5 mA cm^{-2}).

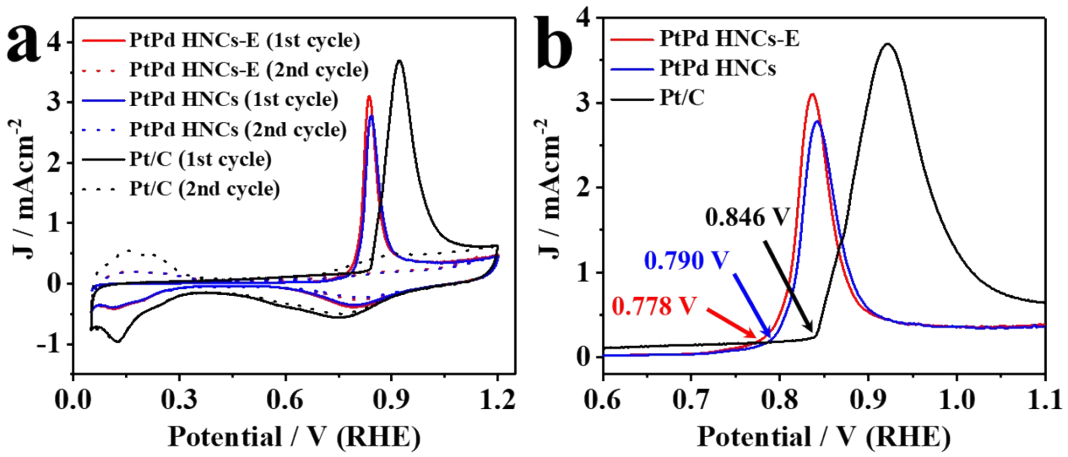

Fig. S8. (a) Original and (b) magnifying CO-stripping voltammograms of PtPd HNCs-E, PtPd HNCs, and commercial Pt/C recorded at 50 mV/s in 0.1 M KOH.

Since CO tolerance ability is a critical parameter for MOR, CO-stripping curves were recorded (Fig. S8). As can be seen, the onset peak potential (0.778 V) of CO oxidation on PtPd HNCs-E is more negative than those on PtPd HNCs (0.790 V) and commercial Pt/C (0.846 V). The lowest voltage means the weakest CO adsorption and best CO tolerance ability of PtPd HNCs-E.[1,2]

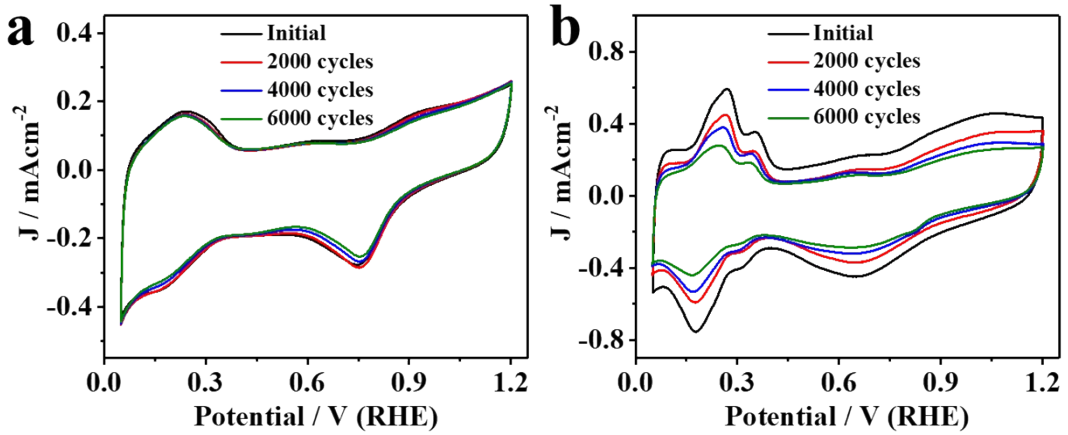

Fig. S9. CV curves of (a) PtPd HNCs-E and (b) commercial Pt/C after different potential sweep cycles.

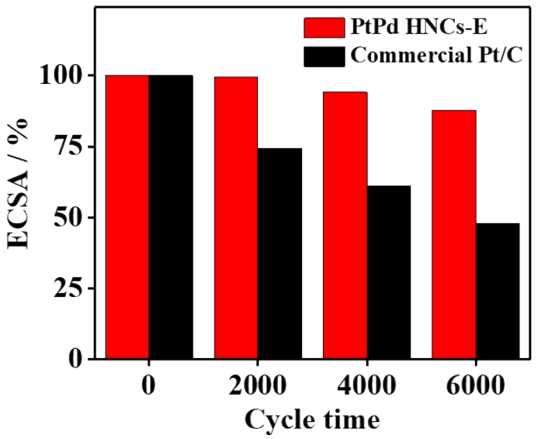

Fig. S10. Loss of ECSA of PtPd HNCs-E and commercial Pt/C after different potential sweep cycles.

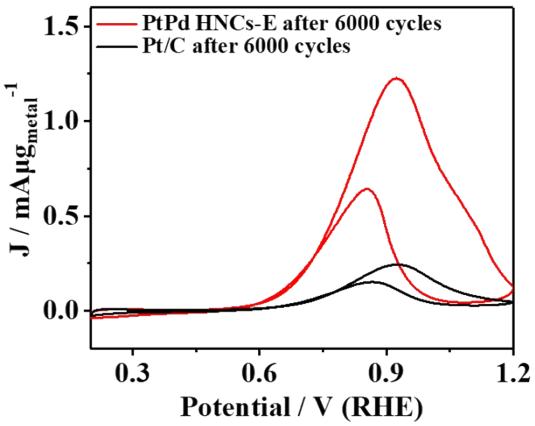

Fig. S11. CV curves of PtPd HNCs-E and commercial Pt/C recorded in 0.1 M KOH + 1 M CH_3OH after 6000 cycles of ADTs.

PtPd HNCs-E exhibited a mass activity of 1.2 mA μg_{metal}^{-1} after 6000 cylces of ADTs, which is 5.0 folds of that for commercial Pt/C (0.24 mA μg_{metal}^{-1}). Moreover, the specific activity of PtPd HNCs-E was 6.3 mA cm^{-2}, which is 6.3 folds of that for commercial Pt/C (1.0 mA cm^{-2}).

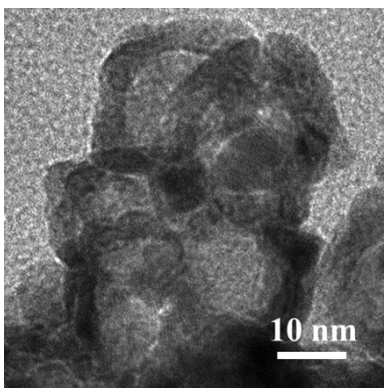

Fig. S12. TEM images of PtPd HNCs-E after 6000 cycles of ADTs.

The morphology of PtPd HNCs-E showed no obvious changes after ADTs.

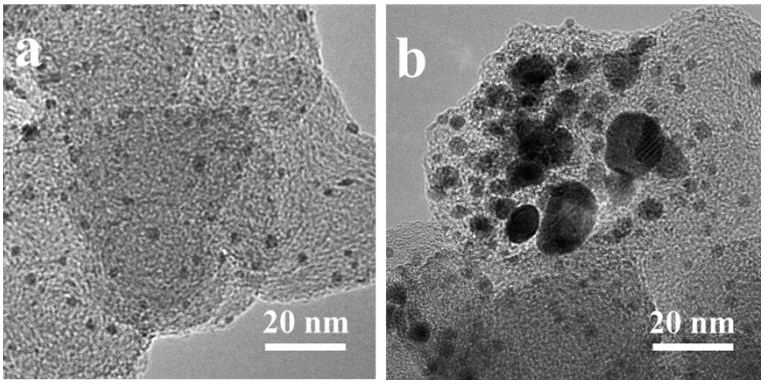

Fig. S13. TEM images of commercial Pt/C (a) before and (b) after 6000 cycles of ADTs.

After 6000 cycles of ADTs, the originally highly dispersed commercial Pt/C (Fig. S15a) turned into heavy aggregation (Fig. S15b).

Table S1. Electrochemical test results of PtPd HNCs-E, PtPd HNCs, and commercial Pt/C.

Sample	**ECSA** (m^2/g_{metal})	**Mass Activity** ($mA/\mu g_{metal}$)	**Specific Activity** (mA/cm^2)
PtPd HNCs-E	25.5	1.7	6.7
PtPd HNCs	23.5	0.89	3.8
Commercial Pt/C	51.7	0.49	0.95

Table S2. Performance of PtPd HNCs-E catalyst in comparison to previously reported novel Pt-based catalysts towards MOR in alkaline conditions.

Catalysts	**Mass activity** ($mA\ \mu g^{-1}$)	**Specific activity** ($mA\ cm^{-2}$)	**References**
PtPd HNCs-E	1.7	6.7	This work
Pt-CoO@NPC@SnO_2	1.52	N.A.	*Appl. Catal. B-Environ.* 2019, **259**, 118043
Pt/karst-Ni	~0.15	~0.037	*Appl. Catal. B-Environ.* 2011, **104**, 382-389
Pt-Ce(CO_3)OH/rGO-2	1.48	2.45	*J. Mater. Chem. A* 2019, **7**, 6562-6571

PtAuRu/RGO/GC	1.6	N.A.	*J. Mater. Chem. A* 2013, **1**, 7255-7261
$Pt/MoS_2/Ni_3S_2$-nrs/NF	0.805	1.05	*ACS Sustainable Chem. Eng.* 2019, **7**, 11101-11109
Pt_1Ni_1/C	~1.75	4.9	*Nano Res.* 2018, **11**, 2058-2068
Pt-Ni-Ir yolk-shell	1.17	2.77	*Nanoscale* 2019, **11**, 23206-23216
AgAu@Pt nanoframes	0.483	1.96	*Nanoscale* 2018, **10**, 2231-2235
Pt-Pd core-shell nanocrystals	N.A.	~0.60	*Nanoscale* 2012, **4**, 845-851
Pt/Te nanorods	0.762	0.90	*Chem. Commun.* 2019, **55**, 11247-11250
Au-Pt yolk–shell	0.086	0.21	*Chem. Commun.* 2011, **47**, 6093-6095
Pt/MC/G	N.A.	0.10	*J. Power Sources* 2011, **196**, 1904-1908
Pt/P-MCNTs	0.835	N.A.	*Catal. Commun.* 2012, 22, 34-38
Au@Pt/MWCNTs	N.A.	4.24	*Catal. Commun.* 2011, **13**, 54-58
Graphene-Pt NP hybrid	1.18	N.A.	*Electrochim. Acta* 2017, **231**, 386-395
rGO-Co_3O_4 modified Pt	N.A.	0.362	*RSC Adv.* 2014, **4**, 62793-62801

N/A*: Not applicable

Table S3. ECSA (m^2/g_{metal}) of PtPd HNCs-E and commercial Pt/C after different potential sweep cycles.

Sample	**Initial**	**2000 cycles**	**4000 cycles**	**6000 cycles**
PtPd HNCs-E	25.5	22.2	21.0	19.6
Commercial Pt/C	51.7	37.1	30.5	24.0

Reference

1 A.-L. Wang, C.-L. Liang, X.-F. Lu, Y.-X. Tong and G.-R. Li, *J. Mater. Chem. A*, 2016, **4**, 1923-1930.

2 Q. Wang, S. Chen, P. Li, S. Ibraheem, J. Li, J. Deng and Z. Wei, *Appl. Catal. B-Environ.*, 2019, **252**, 120-127.